The Conserved Residue Tyrosine 34 Is Essential for Maximal Activity of Iron−Superoxide Dismutase from *Escherichia coli*†

Therese Hunter,‡ Kazunori Ikebukuro,§ William H. Bannister,‡ Joe V. Bannister,‡,|| and Gary J. Hunter*,‡

Department of Physiology and Biochemistry, University of Malta, Msida MSD 06, Malta, Research Centre for Advanced Science and Technology, Tokyo University, 4-6-1 Komaba, Meguro-ku, Tokyo 153, Japan, and Biotechnology Centre, Cranfield University, Cranfield, Bedford MK43 0AL, U.K.

Received December 3, 1996; Revised Manuscript Received February 7, 1997⊗

ABSTRACT: We have expressed, purified, and analyzed the iron-containing superoxide dismutase (FeSOD) of *Escherichia coli* with mutations directed at tyrosine position 34 to introduce phenylalanine (SODY34F), serine (SODY34S), or cysteine (SODY34C). FeSOD and mutant enzymes were purified from SOD-deficient cells using a GST−FeSOD fusion protein intermediate which was subsequently cleaved with thrombin and repurified. Specific activities were measured using the xanthine−xanthine oxidase method and gave 3148 u/mg for wild-type FeSOD. The SODY34S mutation virtually inactivates the enzyme (42 u/mg); mutation to cysteine greatly reduces activity (563 u/mg), but the SODY34F mutant retains nearly 40% of the activity of wild type (1205 u/mg). Fusion protein intermediates were also shown to be active and were demonstrated to protect SOD-deficient *E. coli* cells from the induced effects of oxidative stress, with growth rates directly proportional to the specific activities of the expressed mutant enzymes. S0DY34F exhibited decreased thermal stability, reduced activity at high pH, and a pronounced increase in sensitivity to the inhibitor sodium azide compared with wild-type FeSOD. These results suggest that tyrosine at position 34 is multifunctional and plays a structural role (probably through hydrogen bonding to glutamine at position 69) in maintaining the integrity of the active site, a stabilizing role at high pH, and a steric role in obstructing access to the active site of both substrate and inhibitor molecules.

The superoxide dismutases (EC 1.15.1.1, SOD[1]) are a family of metalloenzymes that together with catalase or peroxidase (Halliwell & Gutteridge, 1985) protect aerobic cells against the detrimental effects of superoxide radicals (O_2^-) (McCord & Fridovich, 1969). Three types of SODs have been described depending on the metal cofactor, copper and zinc (Cu/Zn), manganese (Mn), or iron (Fe) SOD. Cu/ZnSODs, generally located in the cytosol of eukaryotic cells and the chloroplasts of some plants (Bannister et al., 1987), are structurally distinct from the Mn- and FeSODs and utilize the copper ion for catalysis. The Mn- and Fe-containing enzymes are closely related and similar in both structure and amino acid sequence (Parker et al., 1987; Steinman, 1982; Chan et al., 1990; Bannister et al., 1987; Stallings et al., 1991; Parker & Blake, 1988a). MnSOD is common to prokaryotic cells where it is sometimes the sole form of the enzyme and eukaryotes where it is found in mitochondria having been synthesized as a targeted precursor protein (Weisiger & Fridovich, 1973). FeSOD is found in prokaryotic cells, chloroplasts of some plants (Duke & Salin, 1985; Sevilla et al., 1984), and some algae (Kanematsu & Asada, 1979) and protozoa (Michalski & Prowse, 1991). *Escherichia coli* cells contain FeSOD and MnSOD in the cytosol and Cu/ZnSOD in the periplasmic space (Benov et al., 1995). In this bacterium, FeSOD apparently protects proteins and MnSOD protects the nucleoid from damage by superoxide (Hopkin et al., 1992). The role of Cu/ZnSOD is unknown, but it presumably protects cells from environmental superoxide which is unlikely to traverse the cell membrane.

SODs catalyze the dismutation of superoxide in a cyclic redox reaction involving the active site metal cofactor (Fe, Mn, or Cu) (Bull & Fee, 1985; Klug-Roth et al., 1973; McAdam et al., 1977; Stallings et al., 1991). For example, in FeSOD, the reactions are

$$Fe^{3+} + O_2^- \rightarrow Fe^{2+} + O_2 \quad (1)$$

$$Fe^{2+} + O_2^- + 2H^+ \rightarrow Fe^{3+} + H_2O_2 \quad (2)$$

The metal ion is presumed to complex with the superoxide anion as demonstrated by the binding of inhibitors such as azide to Fe(III) in crystals of *E. coli* FeSOD (Stallings et al., 1991; Lah et al., 1995).

Among the 20 FeSOD and 40 MnSOD known complete sequences which vary in length from 190 to 220 amino acids, only 12 residues are absolutely conserved. These include the four ligand binding residues (His 26, His 73, Asp 156, and His 160; *E. coli* numbering is used throughout) and eight other residues (Leu 7, Leu 14, Pro 16, Tyr 34, Trp 122, Trp 158, Glu 159, and Tyr 163). Conservation of a glutamine residue sterically in the active site may also be responsible for the unusual specificity for the metal ion exhibited by such similar proteins (Gln 69 in FeSOD or Gln 146 in

† This work was financially supported by the University of Malta.

* To whom correspondence should be addressed. Telephone: 356-316655. Fax: 356-310577. E-mail: ghun@cis.um.edu.mt.

‡ University of Malta.

§ Tokyo University.

|| Cranfield University.

⊗ Abstract published in *Advance ACS Abstracts,* March 15, 1997.

[1] Abbreviations: SOD, superoxide dismutase; FeSOD and MnSOD, iron- and manganese-containing SOD, respectively; Cu/ZnSOD, copper- and zinc-containing SOD; SODY34F, SODY34S, and SODY34C, *Escherichia coli* FeSOD mutated at tyrosine 34 to phenylalanine, serine, and cysteine, respectively; IPTG, isopropyl β-D-thiogalactopyranoside; NBT, *p*-nitroblue tetrazolium chloride; SDS, sodium dodecyl sulfate; PAGE, polyacrylamide gel electrophoresis; GSH, reduced glutathione; GST, glutathione *S*-transferase.

S0006-2960(96)02954-6 CCC: $14.00

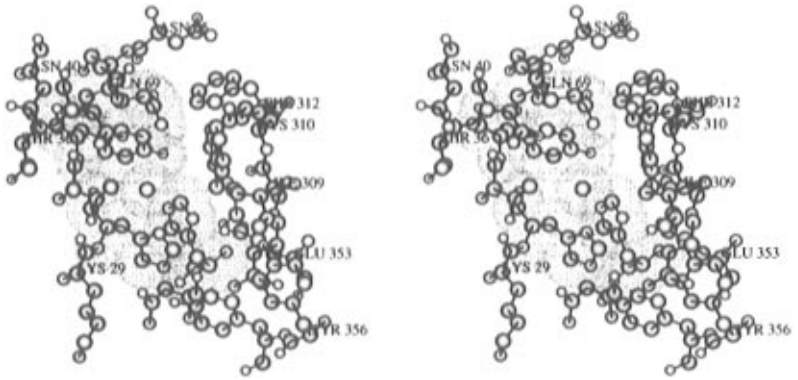

FIGURE 1: Stereoview of the *E. coli* FeSOD active site channel. Ball and stick representation of the residues surrounding the active site Fe^{3+} ion (central sphere surrounded by dots). Residues shown (counterclockwise from the top) are Asn 65, Asn 66, Gln 69, Asn 40, Asn 37, Tyr 34, Thr 36, His 30, Lys 29, His 160, Tyr 357, Tyr 356, Asn 362, Arg 364, Glu 353, Ile 309, Trp 158, Lys 310, and Phe 312. Only some of the residues are labeled (for clarity), and residue numbers above 194 are from the second subunit of the dimer (to the right in this figure). The channel is formed by residues from both subunits, and the path of superoxide substrate (or inhibitor molecules) to the metal ion is blocked to the top by Gln 69 and to the bottom by His 160 (a metal ligand). Tyr 34 and His 30 are in a direct line to the metal. These latter four residues are surrounded by dots at the van der Waals radii of their component atoms. The figure was drawn with coordinates supplied by M. L. Ludwig using MacImdad 5.2 (Molecular Applications Group, Stanford University and Yeda).

MnSOD) (Lah et al., 1995). X-ray crystallographic data of enzymes such as *E. coli* FeSOD (Lah et al., 1995; Stallings et al., 1983), *Bacillus stearothermophilus* MnSOD (Parker & Blake, 1988b), *Pseudomonas ovalis* FeSOD (Stoddard et al., 1990), *Thermus thermophilus* MnSOD (Wagner et al., 1993; Ludwig et al., 1991; Lah et al., 1995), human mitochondrial MnSOD (Borgstahl et al., 1992), and *Mycobacterium tuberculosis* FeSOD (Cooper et al., 1994, 1995) confirm that the iron or manganese cofactor is coordinately bound to five ligands: three histidine residues, one aspartate residue, and a hydroxyl ion. The three-dimensional arrangement of the amino acid ligands approximates to the vertices of a trigonal bipyramid. A sixth coordination position lying between Tyr 34 and His 30 (Figure 1) may become occupied by the substrate during catalysis or by a second hydroxyl at high pH (Lah et al., 1995; Tierney et al., 1995).

The invariant Tyr 34 has been previously implicated in the role of catalysis by participating in substrate interactions, possibly as the proton donor. The phenolic hydroxyl probably forms a hydrogen bond with Gln 69 (Gln 146 in MnSOD), and its aromatic ring may interact with residues hydrophobically (Stoddard et al., 1990; Wagner et al., 1993) (Figure 1). It has also been suggested that the hydroxyl may stabilize the high-pH form of the enzyme (Parker & Blake, 1988b; Tierney et al., 1995).

In FeSOD from *E. coli*, residues from each subunit of the active dimer form a funnel-shaped channel through which substrate molecules must pass to reach the active site metal (Lah et al., 1995). Interrupting the free path to the metal center are residues His 30 and Tyr 34 (Figure 1), each held in place by hydrogen bonding (to Tyr 163 of the opposite subunit and Gln 69, respectively) (Lah et al., 1995). These residues must presumably move aside during catalysis.

We have tested these hypotheses by site-directed mutagenesis of Tyr 34 to phenylalanine, serine, or cysteine.

MATERIALS AND METHODS

Chemicals and Enzymes. Superoxide dismutase (iron-containing enzyme from *E. coli*) and thrombin were purchased from Sigma (Poole, Dorset, U.K.). Xanthine oxidase (from cow milk) and all restriction endonucleases (used according to the manufacturer's instructions in the buffers provided) were purchased from Boehringer Mannheim (Mannheim, Germany). NBT and the Sequenase version 2 kit were obtained from United States Biochemicals (Cleveland, OH). T4 DNA ligase (FPLC *pure*) and GSH−sepharose were purchased from Pharmacia Biotech (Vienna, Austria).

Bacterial Strains and Vectors. The sequencing vector M13mp18 and the expression plasmids pKK223-3 and pGEX-2T were purchased from Pharmacia Biotech. The plasmid pHS1-8, a pBR322 derivative carrying the *sodB* gene from *E. coli*, was a gift from D. Touati, (Institute Jacques Monod, Paris, France). *E. coli* K12 strain TG1 [*sup* E, *hsd* D5, *thi*, Δ(*lac*$^-$ proAB), F'(*tra* D36 *pro* A^+B^+ *lac* I^q *lac* ZDM15)] was supplied with the Oligonucleotide-Directed In Vitro Mutagenesis System from Amersham International, U.K., which was used to generate site-directed mutations. *E. coli* OX326A (Δ *sodA* Δ *sodB*) was kindly supplied by H. Steinman (Albert Einstein College of Medicine, New York).

Oligonucleotide Synthesis. Oligonucleotides were synthesized on an Applied Biosystems model 380B DNA synthesiser using cyanoethyl phosphoramidite chemistry and purified by preparative gel electrophoresis in 20% polyacrylamide containing 7 M urea after which their quality was checked by 5′-end labeling with [γ-^{32}P]ATP and T4 polynucleotide kinase followed by analytical polyacrylamide gel electrophoresis and autoradiography. Before use in mutagenesis protocols, the oligonucleotides were first used as primers in dideoxy sequencing (Sanger et al., 1977) to confirm the position of their unique binding site within the *sodB* gene.

Dideoxy DNA Sequencing. DNA sequencing was carried out by the dideoxy method (Sanger et al., 1977) using Sequenase enzyme. Sequencing of the entire *sodB* gene within the various plasmids and bacteriophage used here was facilitated by the use of an oligonucleotide primer, d(GTTCCAGTAGAAAGTATGGTT), designed to bind to the coding strand 217 nucleotides downstream from the ATG start codon of the *sodB* gene. Double-strand sequencing of pKK223-3 plasmid constructs was performed essentially as described in the manufacturer's protocols (Sequenase sequencing kit) utilizing the oligonucleotide primers PKPRO2, d(TCTCTTCTAAAAGTCGG), and PKTERM, d(TGTGTGGAATTGTGAGC), to prime synthesis in the forward

(− strand as template) and reverse (+ strand as template) directions, as described previously for the vector pKK233-2 (West et al., 1988). Sequencing in pGEX-2T constructs was performed similarly using the oligonucleotide primers PGEX-PLUS, d(GTTTGGTGGTGGCGACCATCCT), and PGEX-MINUS, d(GAGGCAGATCGTCAGCAGTCA).

Construction of M13SODB. The plasmid pHS1-8 (Carlioz et al., 1988) was digested with the restriction endonucleases *Sna*BI and *Cla*I, and the resulting 676 bp fragment (which contained the *E. coli sodB* gene) was purified from an agarose gel by the glass-binding method after performing a filling-in reaction using Klenow DNA polymerase enzyme in the presence of all four nucleotide triphosphates (Sambrook et al., 1989). This fragment was ligated with *Sma*I-cleaved M13mp18 RF DNA and then used to transform *E. coli* TG1 cells made competent by the calcium chloride method (Sambrook et al., 1989). Positive M13 bacteriophage plaques were identified by blue/white selection in the presence of IPTG and 5-bromo-4-chloro-3-indolyl β-D-galactoside. Confirmation and orientation of the inserted *sodB* gene fragment was determined by dideoxy sequencing of positive clones.

In Vitro Site-Directed Mutagenesis. Oligonucleotide site-directed mutagenesis was carried out by the phosphorothioate DNA method of Eckstein (Taylor et al., 1985) utilized in the oligonucleotide-directed *in vitro* mutagenesis system (version 2) from Amersham International, U.K. The oligonucleotides used were d(TAGTGACAAAAGTCTGA) to generate mutant SODY34F and the 2-fold degenerate d(TAGTGACA[G/C]AAGTCTGA) to generate mutants SODY34S and SODY34C simultaneously, using M13*SODB* single-stranded DNA as template. Selection of mutant M13 clones was by dideoxy sequencing.

Construction of pKKSOD2, pKKSODY34F, pKKSODY34S, and pKKSODY34C. M13 RF DNA from each of the *sodB* gene mutants produced by site-directed mutagenesis in M13SOD was digested with the restriction endonucleases *Sac*I and *Pst*I. The DNA was made blunt-ended by treatment with T4 DNA polymerase (Sambrook et al., 1989), and the 705 bp fragments from each clone (containing the *sodB* gene) were isolated by agarose gel electrophoresis and purified by the glass-binding method. This was subsequently used for ligation with the expression plasmid pKK223-3 which had been linearized by digestion with *Sma*I. After competent *E. coli* TG1 cells were transformed with the ligation products, positive clones were selected by plasmid DNA size estimation in agarose gels after total nucleic acid preparation from single colonies (Sambrook et al., 1989). Orientation of the inserted DNA in each expression clone was determined by dideoxy sequencing (Sanger et al., 1977). The wild-type *sodB* gene was similarly subcloned from M13SOD into pKK223-3 and the resulting construct was designated pKK-SOD2 (Figure 2). The constructs of the mutant genes in pKK223-3 were designated pKKSODY34F, pKKSODY34S, and pKKSODY34C. The *sodB* gene of each clone was fully sequenced before use in expression studies.

Construction of pGSOD2, pGSODY34F, pGSODY34S, and pGSODY34C. pKKSOD derivatives (see above) were digested with the restriction endonucleases *Sfu*I and *Bam*HI, and the resultant 635 bp DNA fragment was purified from an agarose gel by the glass-binding method. After end repair using Klenow DNA polymerase enzyme, these fragments were ligated into *Sma*I-digested pGEX-2T. The resultant

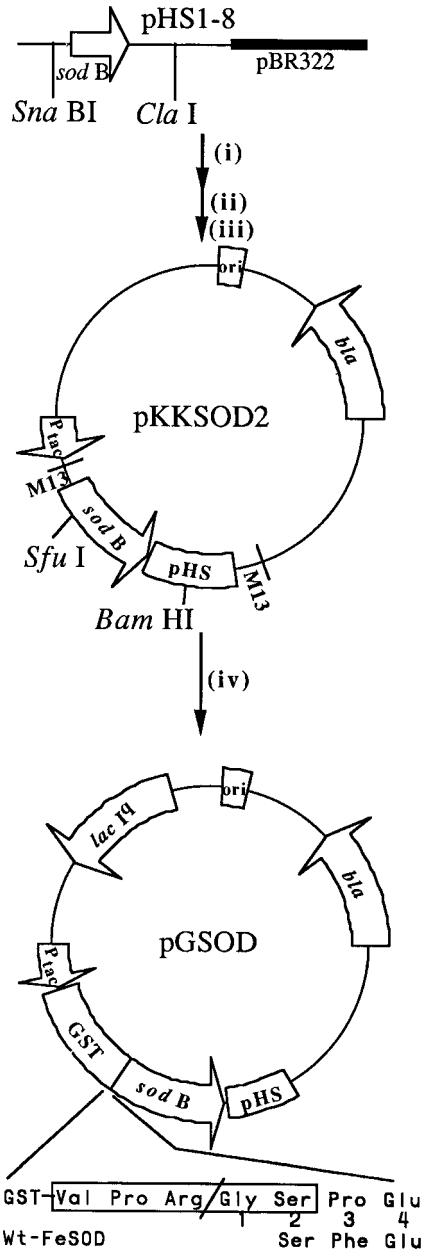

FIGURE 2: Plasmid maps and cloning strategy. A *Sna*BI/*Cla*I DNA fragment containing the *sodB* gene (encoding *E. coli* FeSOD, open arrow) was excised from the clone pHS1-8 (top) (Carlioz et al., 1988) and cloned into the *Sma*I site of M13mp18 (i) for subsequent site-directed mutagenesis (ii). Wild-type and mutated *sodB* genes were subsequently released from the relevant M13 clone by *Sac*I/*Pst*I double digestion and subcloned into the *Sma*I site of the expression vector pKK223-3 to yield pKKSODs (iii) (middle). Regions corresponding to M13 sequences in pKKSOD2 are also indicated. For fusion protein expression, *sodB*-containing fragments from the relevant pKKSOD clone (middle) were isolated by *Sfu*I/*Bam*HI double digestion and cloned into the *Sma*I site of pGEX-2T to give pGSODs (iv) (bottom). The plasmid maps show the origin of replication (ori), the glutathione *S*-transferase gene (GST), and fragments obtained from pHS1-8 (pHS) as labeled open boxes, the ampicillin resistance gene (*bla*), the lac repressor overproducing gene ($lacI^q$), the gene for FeSOD (*sodB*), and the *tac* promoter (P_{tac}) as labeled open arrows in the correct orientation. The sequence of the GST−SOD fusion protein junction is given below the map of pGSOD and shows the thrombin recognition site (boxed) and point of cleavage (slash between Arg and Gly). Numbers indicate the first four amino acids of the purified FeSODs used in this study. The N-terminal sequence of authentic *E. coli* FeSOD is also shown (Wt-FeSOD). The figure is not to scale; see Materials and Methods for details.

plasmids were designated pGSOD2, pGSODY34F, pGSODY34S, and pGSODY34C (Figure 2).

Expression from the sodB Gene in pKKSOD and pGSOD Clones. *E. coli* TG1 cells transformed with the pKKSOD derivatives and *E. coli* OX326A (Δ *sodA* Δ *sodB*) harboring the pGSOD plasmids were grown in 50 mL shaking cultures at 37 °C in 2TY medium (1.6% tryptone, 1% yeast extract, and 0.5% sodium chloride) supplemented with 100 μg/mL ampicillin, sodium salt, and 50 μM ferric sulfate. When the OD_{600} of the culture reached a value of 0.3, IPTG was added to a final concentration of 10 mM and the culture incubated for a further 6 h. Cells were then harvested by low-speed centrifugation and resuspended in approximately 5 mL of KP buffer (50 mM potassium phosphate and 0.1 mM EDTA at pH 7.8). All sample volumes were then adjusted to give an equal OD_{600}. Resuspended cells (1 mL aliquots) were disrupted by sonication at an amplitude of 14 μm for six 30 s bursts over 6 min. Sonic extracts were stored at −80 °C.

Protein Purification. After centrifugation, OX326A-[pGSOD] cells were resuspended in a final volume of 4 mL of PBS buffer (20 mM sodium phosphate buffer at pH 7.2 and 150 mM sodium chloride) and lysed by passage through a French Press (Amicon) at 16 000 psi. The cell lysates were centrifuged at 12000*g* for 2 min and filtered through a 0.45 μm Nalgene filter, and the filtrates were loaded onto prepacked GSH−sepharose columns (2 mL) obtained from Pharmacia. Unbound protein was washed through the column with 20 mL of PBS. GSH (10 mM) in Tris-HCl (50 mM, pH 8.0) was used to elute the bound fusion protein. Fractions of 750 μL were collected, and GST−FeSOD was detected in fractions 2−4. Fusion proteins were digested with thrombin in the presence of 1 mM $CaCl_2$ at room temperature. GST was removed by passage through a GSH−sepharose column as described above, and SOD was collected in the through-wash. GST−SOD fusion proteins and FeSODs were dialyzed against KP buffer, concentrated using Microcon 30 instruments (Amicon), and stored at −80 °C.

Assay for Superoxide Dismutase Activity. Activity of SOD was measured spectrophotometrically by its inhibitory action on the superoxide−dependent reduction of cytochrome *c* by xanthine-xanthine oxidase as described by McCord and Fridovich (1969) and Ysebaert-Vanneste and Vanneste (1980). The reduction of cytochrome *c* was followed at a wavelength of 550 nm using a Beckman diode array DU7500 spectrophotometer in KP buffer at 25 °C and a final volume of 1 mL. A blank measurement was recorded in the absence of sample over 1 min (V_b). Sample volumes of 200−5000-fold dilutions of the sonic extracts ranged from 0.1 to 0.5 mL, and cytochrome *c* reduction was followed over 1 min (V_s) for each sample volume. The slope of a plot of the reciprocal of the sample volume against V_b/V_s was used to calculate SOD activity (Ysebaert-Vanneste & Vanneste, 1980). Specific activity was also measured using 50 mM potassium carbonate and 0.1 mM EDTA buffer at pH 11. All assay constituents were dissolved in this buffer before use, and the amount of xanthine oxidase required was adjusted to give a blank value (V_b) of 0.025 Δ*A*/min.

Thermal Stability Studies. Thermal stability was studied by incubating either FeSOD (0.9 μg/mL) or SODY34F (2.36 μg/mL) in KP buffer at different temperatures (25, 37, 40, 45, 50, 55, 60, 65, and 70 °C) for 45 min or at 50 °C for different time intervals. Samples (250 μL) were removed and kept immediately on ice until residual SOD activity was measured at 25 °C. The addition of 200 μL of each sample to a standard reaction mixture of 1.0 mL gave identical activities for each of the enzymes at the dilutions given above prior to incubation. Residual activities were expressed as a percentage.

Effect of Sodium Azide. Different concentrations of the inhibitor sodium azide were prepared in KP buffer, and 10 μL of each was added to SOD assay mixtures prior to the addition of xanthine oxidase (1.0 mL final volume). Concentrations of FeSOD and SODY34F and assay conditions were as reported for thermal stability studies.

Polyacrylamide Gel Electrophoresis (PAGE). Native 8% polyacrylamide gels (29:1 acrylamide:N,N′-methylenebisacrylamide) containing Tris-HCl pH 8.8 utilized a Tris-glycine electrophoresis buffer system consisting of 25 mM Tris and 250 mM glycine at pH 8.3. Samples contained 50 mM Tris-HCl (pH 6.8), 0.1% bromophenol blue, and 10% glycerol prior to gel application. Denaturing polyacrylamide gel electrophoresis (SDS−PAGE) was carried out in 15% polyacrylamide gels essentially by the procedure of Laemmli (1970) utilizing a 5% stacking gel. Samples were pretreated by boiling for 4 min in 100 mM Tris-HCl (pH 6.8), 100 mM DTT, 2% SDS, 0.1% bromophenol blue, and 10% glycerol prior to application to the gel.

Superoxide Dismutase Activity Stain. Native PAGE gels were stained for SOD activity by the NBT reaction as described by Beauchamp and Fridovich (1971).

Protein Concentration. Estimation of the concentration of protein in sonic extracts was by the method of Lowry et al. (1951) using bovine serum albumin as the standard.

N-Terminal Sequencing of Purified FeSOD. The N-terminal sequence of purified FeSOD was determined with a Porton Instruments PI 2090E Integrated Microsequencing System and a Beckman System Gold high-performance liquid chromatograph connected on-line to a Beckman 168 diode array detector.

Protection against Paraquat-Induced Stress. Overnight cultures (5 mL) of *E. coli* OX326A transformed with the appropriate plasmid were diluted 1:100 in 2TY medium to a final volume of 5 mL, grown with shaking at 37 °C for 1−2 h, and used to inoculate 50 mL of 2TY media containing 100 μg/mL ampicillin, 50 μM ferric sulfate, 250 μM paraquat, and 0.1 mM IPTG to an initial OD_{600} of 0.03. Cultures were grown in 250 mL flasks with shaking at 37 °C, and 1 mL aliquots were removed regularly to measure optical density.

RESULTS

Mutation of Tyrosine 34. All Fe- and MnSODs contain a conserved tyrosine residue at position 34 (*E. coli* numbering) which is understood from structural analyses to occupy a critical position in the active site of these enzymes (Figure 1, Discussion). The *sodB* gene from *E. coli* was subcloned from the plasmid pHS1-8, a pBR322 derivative (Figure 2) into M13mp18 in which site-directed *in vitro* mutagenesis was carried out to produce M13SOD clones containing wild-type (FeSOD) and mutant (SODY34F, SODY34S, and SODY34C) *sodB* genes (Materials and Methods). The introduction of mutations was confirmed by dideoxy DNA sequencing (Materials and Methods, results not shown).

Expression of pKKSOD Derivatives. In order to achieve high levels of expression of wild-type and mutant FeSODs, the wild-type and mutant genes were subcloned from the appropriate M13SOD clone into the vector pKK223-3 where

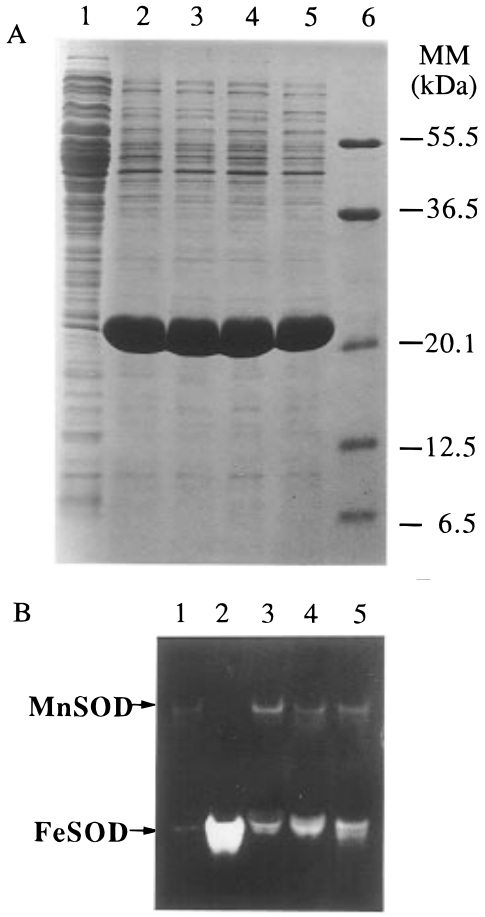

FIGURE 3: Expression of superoxide dismutase (SOD) mutants from pKK223-3. (A) Sonic extracts of *E. coli* TG1 cells harboring the appropriate expression plasmid (10 μg of total protein) were loaded in each lane of a 15% SDS−polyacrylamide gel. In lane 1, cells contained the vector pKK223-3 and in lane 2 pKKSOD2 (wild-type), and lanes 3−5 contained the mutants pKKSODY34F, pKKSODY34S, and pKKSODY34C, respectively. In each case, protein expression was induced by 10 mM IPTG as described in Materials and Methods. Molecular mass markers (MM) were applied to lane 6. (B) Native PAGE (8%) stained for SOD activity. Forty micrograms of total protein of sonic extracts was loaded in each of the lanes in the same order as above for panel A.

they came under the control of the inducible *tac* promoter (Materials and Methods, Figure 2). All pKKSOD clones were characterized by dideoxy DNA sequencing, during which the entire *sodB* gene sequence was confirmed (results not shown).

Sonic extracts of *E. coli* TG1 cells transformed with the expression constructs pKKSOD2, pKKSODY34F, pKKSODY34S, and pKKSODY34C (which express wild-type FeSOD, SODY34F, SODY34S, and SODY34C, respectively, Materials and Methods) that had been induced by the addition of IPTG (10 mM) were analyzed for protein production and SOD activity by PAGE. SDS−PAGE (Figure 3A) of the lysates shows the high level of expression from each of the clones in this system as indicated by the large protein band present in each extract (lanes 2−5, Figure 3A) corresponding to a molecular mass of approximately 21 000 Da, the same as that of authentic FeSOD protein. When IPTG was omitted from the growth media, expression of this protein band was considerably reduced (results not shown) though significantly greater than that represented by *E. coli* TG1 cells harboring the vector pKK223-3 (lane 1, Figure 3A) and which produce FeSOD *via* expression from the genome. Expression of SODs in TG1 cells was determined to be approximately 4% of the total cell protein in such cells by laser densitometry (results not shown). In contrast, induced cultures of *E. coli* TG1 harboring expression clones (lanes 2−5, Figure 3A) were determined to be producing approximately 62% of the total cell protein, as the 21 000 Da band, by the same method (results not shown). With meticulous control over the growth conditions, variation between the expression of each mutant was kept within 5%, again as measured by laser densitometry of Coomassie-stained SDS−polyacrylamide gels (results not shown). Native polyacrylamide gels subjected to the negatively staining NBT reaction for SOD activity (Beauchamp & Fridovich, 1971) unequivocally demonstrated the overproduction of the enzyme from cells transformed with pKK-SOD2 (lane 2, Figure 3B) when compared with expression from untransformed cells (lane 1, Figure 3B). Mutant FeSOD proteins showed little difference in the levels of activity with this technique and displayed more than one achromatic band in the region expected for FeSOD (lanes 3−5, Figure 3B). One complication of this methodology is the possible interaction of mutant SOD monomers, forming heterodimeric proteins with wild-type enzymes expressed in *E. coli* TG1 cells (lane 1, Figure 3B). In cells expressing mutant proteins, active heterodimers may be formed between wild-type and mutant FeSOD as well as between mutant and MnSOD, although genomic expression of both FeSOD and MnSOD is usually low (lane 1, Figure 3A). Furthermore, it can be seen from Figure 3B that the expression of MnSOD (inducible by conditions of stress) is increased in cells expressing mutant enzymes (lanes 3−5, Figure 3B) compared to that in cells containing vector alone (lane 1, Figure 3B) and that cells overexpressing wild-type FeSOD express almost no MnSOD (lane 2, Figure 3B).

The specific activities of the various mutant enzymes expressed in TG1 cells are given in Table 1. Background expression of both FeSOD and MnSOD in these cells was measured to be 24 u/mg, and this value was subtracted from the values obtained for overexpressing cells before normalizing the values (last column in Table 1). SODY34F showed almost one-third of the activity of wild-type FeSOD; SODY34C had approximately one-fifth of the activity of wild-type FeSOD, and SODY34S was the least active of the mutant enzymes with only one-twentieth of the activity of wild type. Due to the observed differences in activity observed on PAGE (Figure 3B) and because of the complications inherent in this system, we decided to express and purify the mutant enzymes using SOD-deficient cells.

Expression of pGSOD Derivatives. The wild-type and each mutant FeSOD gene were subcloned from the appropriate pKKSOD clone into the GST fusion protein expression vector pGEX-2T as described in Figure 2 (Materials and Methods). Again, the *sodB* gene was completely sequenced by the dideoxy method in each clone to ensure the incorporation of only one mutation and to confirm that the DNA sequence at the junction between the GST and SOD genes was correct (see below). These constructs expressed GST−SOD fusion proteins also under the control of the *tac* promoter. Expression, however, was much more tightly controlled in these constructs due to the presence in this vector of the *lac*I^q gene (Figure 2). Figure 4A shows the expression of the fusion proteins from these clones in *E. coli* OX326A (Δ *sodA* Δ *sodB*) cells which correspond to the predicted molecular mass of 47 300 Da (lanes 2−6, Figure 4A). Fusion proteins constituted approximately 32% of the

Table 1: Specific Activities of the Crude and Purified FeSODs

cell type and expression plasmid	protein expressed	SOD activity[a] (u/mg)	SOD activity[b] normalized (%)
TG1 [pKK223-3]	none, crude lysate	24 ± 3	–
TG1 [pKKSOD2]	FeSOD, crude lysate	1459 ± 229	100
TG1 [pKKSODY34F]	SODY34F, crude lysate	456 ± 73	31
TG1 [pKKSODY34C]	SODY34C, crude lysate	300 ± 11	21
TG1 [pKKSODY34S]	SODY34S, crude lysate	74 ± 11	5
OX326A [pGSOD]	GST−FeSOD, pure	1428 ± 31	100
OX326A [pGSODY34F]	GST−SODY34F, pure	449 ± 37	31
OX326A [pGSODY34C]	GST−SODY34C, pure	240 ± 30	17
OX326A [pGSODY34S]	GST−SODY34S, pure	12 ± 5	1
OX326A [pGSOD]	FeSOD, pure	3148 ± 50	100
OX326A [pGSODY34F]	SODY34F, pure	1205 ± 243	38
OX326A [pGSODY34C]	SODY34C, pure	563 ± 50	18
OX326A [pGSODY34S]	SODY34S, pure	42 ± 5	1

[a] Activity of SOD as measured by xanthine−xanthine oxidase assay. Results are shown as the mean from at least three individual measurements. [b] SOD activity normalized to 100% in each of three separate experiments: expression in TG1 cells using crude cell lysates, purified GST−SOD fusion proteins, and purified SOD proteins.

total protein in these cells, as measured by laser densitometry of Coomassie-stained SDS−polyacrylamide gels (results not shown). Purification of these fusion proteins was carried out on Glutathione−Sepharose columns (Materials and Methods) and yielded a protein of the expected size (lane 7, Figure 4A). The junction between the GST moiety and SOD in the fusion proteins is shown in Figure 2 which illustrates the recognition site for the restriction protease thrombin. After treatment of the fusion proteins with this protease, both GST (molecular mass of 26 100 Da) and SOD (molecular mass of 21 100 Da) were observed by SDS−PAGE (lane 8, Figure 4A). Further purification by Glutathione−Sepharose affinity chromatography was used to remove the released GST protein to leave pure SOD (lanes 9−12, Figure 4A) with the same mobility as authentic FeSOD from Sigma (lane 13, Figure 4A). The N-terminal sequence as predicted from the cloning strategy, however, of the FeSOD enzymes purified by this methodology, was slightly different from that of authentic FeSOD (Figure 2) and was confirmed by both DNA sequencing the plasmid constructs and N-terminal sequencing purified FeSOD by Edman degradation (results not shown).

The activity of SOD in both the purified GST−SOD fusion proteins and the purified SODs was investigated by PAGE (Figure 4B). Only the wild-type fusion protein construct showed detectable activity by this method under the conditions used (lanes 1−4, Figure 4B). When larger quantities of the fusion proteins were loaded, the gels showed aberrant red staining in the position of the fusion proteins (results not shown). Purified SODs however all showed some activity, which approximated the measured activities reported for expression in TG1 cells (lanes 6−9, Figure 4B, Table 1). Purified SODs did not demonstrate mobilities in PAGE significantly different from that of authentic wild-type FeSOD (lane 10, Figure 4B).

Specific activities of the wild-type and mutant enzymes were measured in purified protein preparations of both GST−SOD fusion proteins and SODs (Table 1). Relative activities between wild-type and mutant enzymes are not significantly different from those reported for activities measured in crude lysates of TG1 cells (Table 1). The differences observed in specific activities measured for purified fusion proteins and purified SODs reflect the difference in size between the two protein types; the larger GST−SOD fusion proteins show a reduced specific activity compared to purified SODs (Table 1).

Protection against Paraquat-Induced Stress. It was found that pKKSOD and mutant derivatives would not produce transformants of *E. coli* OX326A (Δ *sodA* Δ *sodB*), presumably because of the high expression of protein even in the absence of IPTG (results not shown). Experiments to demonstrate the protection of SOD-deficient cells under oxidative stress by each mutant FeSOD were therefore carried out using the fusion constructs pGSOD, pGSODY34F, pGSODY34S, and pGSODY34C.

Oxidative stress was induced in *E. coli* cultures by the addition of paraquat, a herbicide which produces superoxide anions intracellularly *via* the electron transport chain (Hassan & Fridovich, 1978). All inoculants were grown in the absence of both paraquat and IPTG to achieve exponential growth rates prior to stress and protein induction. Growth of OX326A cells was significantly reduced in the presence of paraquat (250 μM) compared to that in its absence (Figure 5, closed and open circles, respectively). The introduction of the vector pGEX-2T into these cells resulted in a further decrease in growth rates both in the absence and in the presence of paraquat (Figure 5, open and closed squares, respectively), presumably due to the increased stress of producing plasmid-encoded proteins such as β-lactamase necessary for plasmid maintenance in cultures containing ampicillin (Materials and Methods). OX326A cells expressing wild-type FeSOD from the plasmid pGSOD exhibited almost the same growth rates with and without paraquat (Figure 5, closed and open triangles, respectively) when protein expression was induced with 0.1 mM IPTG (Materials and Methods). Various growth rates were obtained when OX326A cells harboring the mutant SOD proteins were grown under similar conditions (Figure 5). Interestingly, the observed growth rates correlated in direct proportion with the measured SOD activities of the enzyme expressed by the plasmid construct (Figure 5, inset). Simply put, the higher the specific activity of SOD expressed, the faster the growth rate of the cell in the presence of induced oxidative stress.

Effects of Temperature on Enzyme Activity. Because of its unexpectedly high activity and the significance of the mutation, SODY34F was chosen for further characterization. The thermal stability of purified proteins was investigated both with time at 50 °C (Figure 6A) and at different temperatures when incubated for 45 min (Figure 6B). Comparison with FeSOD purified *via* the same route (see above) is striking. The profile of SOD activity (measured

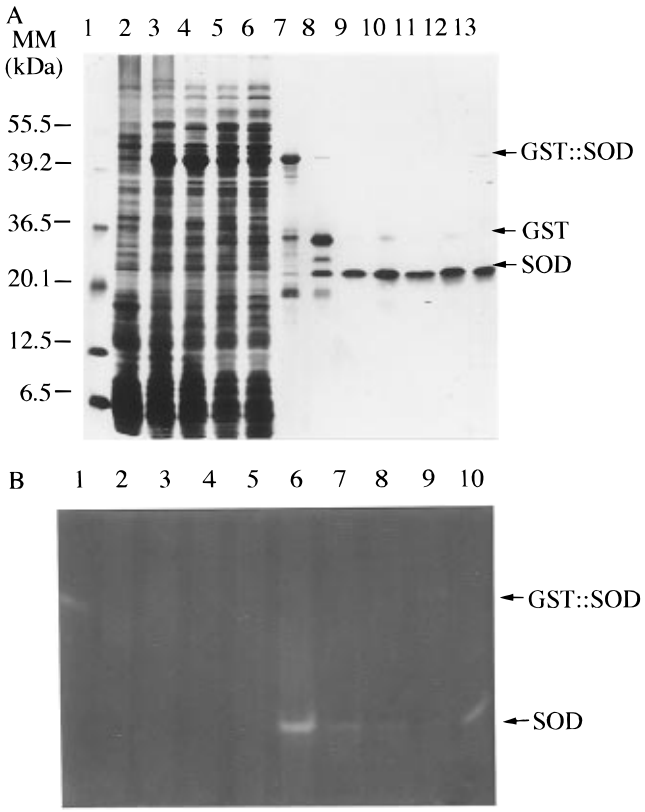

FIGURE 4: Expression and purification of GST−SOD fusion proteins. After induction with 10 mM IPTG, cells harboring the appropriate plasmid were lysed by passage through a French pressure cell. (A) Samples (10 μg of total protein) were resolved by 15% SDS−PAGE and silver-stained. Lane 1 contained the molecular mass markers (MM), lane 2 extracts of *E. coli* OX326A harboring the plasmid pGEX-2T, and lanes 3−6 extracts of *E. coli* OX326A harboring the plasmids pGSOD, pGSODY34F, pGSODY34S, and pGSODY34C, respectively. Lane 7 contained 4 μg of GST−FeSOD fusion protein purified by GSH−sepharose chromatography; lane 8 is a thrombin-cleaved GST−FeSOD sample, and lanes 9−12 were the subsequently rechromatographed, purified FeSOD, SODY34F, SODY34S, and SODY34C, respectively. Lane 13 contained 5 μg of *E. coli* FeSOD from Sigma. Positions of GST−SOD fusion protein, GST, and SOD are indicated by arrows to the right of the figure. (B) Native PAGE (8%) stained for SOD activity. Ten micrograms of protein was loaded in each lane. Lane 1 contained purified GST−FeSOD (wild-type), lane 2 GST−SODY34F, lane 3 GST−SODY34S, and lane 4 GST−SODY34C. Lane 5 contained GST alone. FeSOD proteins purified by thrombin cleavage and rechromatography on GSH-sepharose were applied to lanes 6−9 (FeSOD, SODY34F, SODY34S, and SODY34C, respectively). Five micrograms of FeSOD from Sigma was applied to lane 10. Positions of GST−SOD and purified SOD are indicated by arrows to the right of the figure.

at different times during incubation of the enzymes at 50 °C, Figure 6A) demonstrates unequivocally the decreased thermal stability of the SODY34F mutant. SOD activity decreases drastically with time; after 45 min, activity of SODY34F has reduced to approximately 25%. This compares with a reduction to about 80% for FeSOD. Similarly, when SOD activity is measured after incubation of the enzymes at different temperatures (Figure 6B), a pronounced difference between the enzymes is observed. SODY34F exhibits a rapid reduction in enzyme activity between 45 and 50 °C, whereas FeSOD was found to exhibit a similar reduction between 55 and 60 °C (Figure 6B). These results may be indicative of the role played by hydrogen bonding of the phenolic hydroxyl of Tyr 34 to Gln 69 in FeSOD, probably in maintaining the structural integrity of the protein.

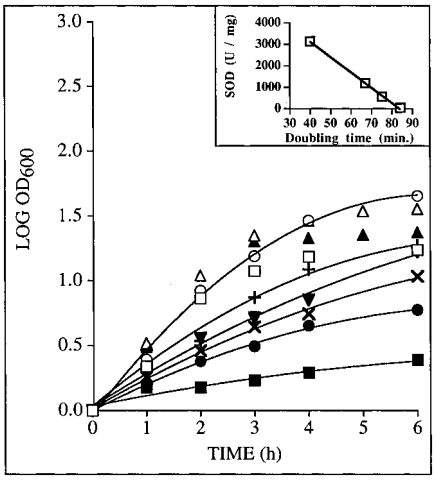

FIGURE 5: Effect of mutant SODs expressed in *E. coli* OX326A (Δ *sodA* Δ *sodB*) cells under paraquat-induced stress. *E. coli* OX326A (Δ *sodA* Δ *sodB*) cells harboring the appropriate plasmid were grown to exponential phase and used to inoculate media containing IPTG (0.1 mM) and paraquat (250 μM). Cell growth was followed by measuring the optical density at 600 nm. Open symbols indicate the absence of paraquat in the growth medium: pGEX-2T vector (□), OX326A cells with no plasmid (○), pGSOD (△), pGSODY34F (+), pGSODY34S (×), and pGSODY34C (▼). Curves for the data points shown for pGEX-2T and pGSOD cells without paraquat (□ and △, respectively) and for pGSOD under stress (▲) have been omitted for clarity. The inset figure shows the linear relationship between doubling time (as measured from the initial rates in the growth curves) and SOD specific activity for each mutant FeSOD.

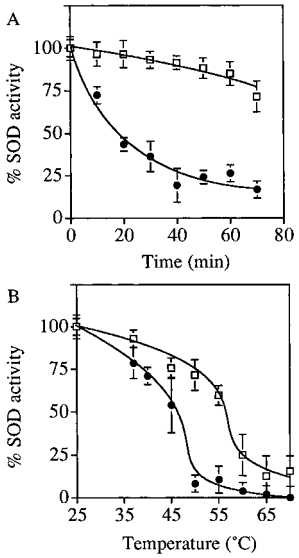

FIGURE 6: Effect of temperature on the activity of FeSOD and SODY34F. Samples of purified FeSOD and SODY34F were adjusted to give 1 unit of SOD activity under standard assay conditions. Changes in the observed activity, measured at 25 °C after incubation, were normalized to this as a percentage. (A) Aliquots were held at 50 °C for the indicated times before being assayed. (B) Aliquots were held at the indicated temperatures for 45 min before being assayed. Each data point is the result of three individual measurements for FeSOD (□) and SODY34F (●).

Azide Inhibition. The effects of the SOD inhibitor sodium azide were also shown to be capable of discriminating between FeSOD and SODY34F (Figure 7). SODY34F exhibited a 20-fold higher affinity for azide (dissociation constant, K_d, of 0.1 mM) compared to FeSOD (K_d of 2 mM) (Figure 7). Azide is known to approach the FeSOD active site *via* the same route as the superoxide substrate (Stallings et al., 1991; Lah et al., 1995). As residue Tyr 34 projects

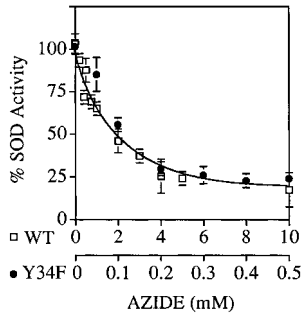

FIGURE 7: Effect of azide on the activity of wild-type FeSOD and FeSODY34F. Samples of purified FeSOD and SODY34F were adjusted to give 1 unit of SOD activity under standard assay conditions. Changes in the observed activity in the presence of azide were normalized to this as a percentage. Aliquots of each SOD were added to the appropriate volume of sodium azide and assayed immediately. Each data point is the result of three individual measurements for FeSOD (WT, □) and SODY34F (Y34F, ●). Note that the horizontal axes have a different scale for each SOD. The axis for FeSOD (WT) indicates azide concentrations 20 times that used for SODY34F (Y34F) to give similar response curves.

into this path near the metal ion at the active site, the differential effects of azide observed are presumably the result of steric hindrance in FeSOD and a reduction of it in the mutant SODY34F.

Effects of pH on Enzyme Activity. The specific activities of both FeSOD and SODY34F were measured at elevated pH. A comparison of the activity of the FeSOD enzyme at pH 7.8 and 11 showed an increase of approximately 50% to 4789 ± 585 u/mg. This may be attributable to some extent to the different buffer system used (see Materials and Methods). In contrast, the specific activity of the mutant SODY34F exhibited a decrease of approximately 60% at pH 11 to 469 ± 17 u/mg. Presumably, this dramatic difference between the two SODs is due to the ionization of the phenolic hydroxyl of Tyr 34 ($pK_a \sim 10$), a reaction which may stabilize the protein structure in some way at high pH (Fee et al., 1981a; Lah et al., 1995; Tierney et al., 1995).

DISCUSSION

In the crystal structure of Fe- and MnSODs, a channel is formed through which the superoxide substrate (O_2^-) or anionic inhibitors (such as azide, N_3^-) must pass to reach the Fe^{3+} ion at the center of the active site (Figure 1) (Ludwig et al., 1991; Stallings et al., 1991; Lah et al., 1995). In the FeSOD of *E. coli*, this channel is made up of amino acid residues from both subunits of the active dimer (Figure 1) (Lah et al., 1995). Between the channel and the Fe^{3+} ion lie residues His 30, Tyr 34, and His 160. The latter is a metal ligand and is presumably effectively immobile, whereas in the dynamic enzyme in solution, both His 30 and Tyr 34 are probably capable of considerable motion as has been implied by Brownian dynamics simulation (Sines et al., 1990). These latter studies and others have also shown that the residues of the channel (Figure 1) carry surface charge distributions which would serve to steer the superoxide toward the active site where it would need to approach the Fe^{3+} to within 4.5 Å for dismutation to take place (Sines et al., 1990; Benovic et al., 1983). Such fluctuations in active site and channel motion have also been modeled in the Cu/ZnSOD enzyme (Shen et al., 1989). In agreement with these results is the structural analysis of azide complexed with FeSOD where the N_3^- ion takes up a position 2.12 Å from the Fe^{3+} ion to which it has become complexed as a sixth ligand parallel to and approximately in the plane of the ring atoms of Tyr 34 (Lah et al., 1995). This geometry has led to the speculation that azide acts as a superoxide mimic and that superoxide, too, takes up a sixth coordination position to the Fe^{3+} (Lah et al., 1995) during catalysis.

We have investigated the effect of mutations in the invariant tyrosine residue at position 34 of *E. coli* FeSOD on enzyme activity. These mutations effectively remove the phenolic hydroxyl but leave the aromatic ring intact (SODY34F) or remove the phenolic hydroxyl and the aromatic ring (SODY34S and SODY34C). GST−SOD fusion proteins were produced in SOD-deficient *E. coli* from which highly purified FeSOD and mutant SOD enzymes were obtained after processing (Figure 4). Although only GST−FeSOD showed activity on native PAGE (Figure 4B), purified GST−SOD fusion proteins, demonstrated activities which approximately paralleled those observed in pKKSOD constructs measured in crude lysates (Table 1). All purified SODs were active on native PAGE (lanes 6−9, Figure 4B), and the N-terminal amino acid changes (Figure 2) had no apparent effect on the activity of FeSOD. Relative activities of purified SOD mutants also paralleled closely the activities of the fusion proteins (Table 1); differences in specific activities were found to be due only to the increased size of the fusion proteins.

Importantly, the SODY34F mutant was shown to be nearly 40% as active as wild-type FeSOD (1205 u/mg), whereas the SODY34S mutant was almost inactive (42 u/mg). This provides strong evidence for an involvement of the hydroxyl group of Tyr 34 as well as a significant contribution of the aromatic ring toward activity. Although the SODY34C mutant showed activity somewhere between that of SODY34S and SODY34F (563 u/mg), interpretation of this result is difficult due to the possible interaction of the thiol group with superoxide. We provide evidence that Tyr 34 plays a multifunctional role. Thermal stability of the SODY34F mutant was greatly reduced compared to that for FeSOD (Figure 6). Sensitivity to azide inhibition was shown to be 20-fold greater for the mutant SODY34F ($K_d = 0.1$) than for FeSOD ($K_d = 2.0$, Figure 7). Values for K_a for azide have been reported as 1−2 mM, and K_d for azide has been reported as 4−20 mM (Fee et al., 1981a). The structure of FeSOD is relatively insensitive to changes in pH, particularly high pH, although different methods for measuring any effect make comparison difficult. Changes in the spectral properties of the enzyme have indicated an ionizing group with an apparent pK_a of approximately 9 which was assigned tentatively to hydrolysis of bound water (Fee et al., 1981a). Stopped-flow spectrophotometry also revealed a group involved in catalysis which ionizes with a pK_a of ∼8.8 (Fee et al., 1981b). X-ray absorption spectroscopy has shown a high-pH transition consistent with an increase in the coordination number of the active site iron from five to six and an approximate pK_a of 9.8 (Tierney et al., 1995). In our assays, FeSOD specific activity was found to increase by 50%, whereas the activity of SODY34F was found to decrease by 60%.

These findings are no doubt due in some part to the hydrogen bonding known to occur between the hydroxyl group of Tyr 34 and Gln 69 (Figure 1), although interactions involving other residues cannot be altogether ruled out. These results are also in excellent agreement with the known dynamics of azide binding to the FeSOD enzyme. It is not unreasonable to suppose that the absence of the Tyr 34

phenolic hydroxyl in SODY34F makes the metal ion more easily accessible to the azide ion. This effect may also be enhanced by the fact that, as well as removing a steric hindrance to azide approaching the active site, the hydrogen bond between Tyr 34 and Gln 69 cannot be formed and the capability of Phe 34 to flip dynamically out of the approach path to the metal ion is subsequently improved.

In vivo protection of SOD-deficient cells under induced oxidative stress was demonstrated by the GST−SOD fusion proteins (Figure 5). We have shown that, when under oxidative stress, the specific activities of the mutant enzymes are directly proportional to the growth rates of the SOD-deficient cells expressing them (Figure 5, inset). This result shows that the GST moiety of the fusion proteins has no obvious physiological effect and that the measurement of growth rates under carefully controlled conditions may be a simple alternative to the measurement of relative enzyme activities for SOD mutant proteins. Perhaps more importantly, this result leads us to believe that, for a similar amount of protein expressed in different cell types, the degree of protection afforded against oxidative stress will be directly related to the enzyme's specific activity. Although this statement seems obvious, evidence of this effect with SOD has not been reported previously to our knowledge. This may indicate that, in comparisons of cellular growth under induced oxidative stress, measurements of SOD protein expression is not enough and that specific activities must be measured or taken into account, particularly where different types of SOD are involved.

The unexpectedly high activity of the SODY34F mutant enzyme is curious as no Fe- or MnSOD has been found with any residue other than tyrosine in this position. Considering the ability of the SODY34F mutant to protect cells physiologically (Figure 5), one might have expected such a change to have taken place at some time during the evolution of these enzymes. The reduced activity of this mutant might be compensated by higher expression levels in cells under stress. The exceptional sensitivity of the SODY34F mutant to heat, azide, and pH may help explain the absence of such a mutant in nature.

ACKNOWLEDGMENT

We thank Prof. D. Touati and Prof. H. Steinman for the gifts of plasmid pHS1-8 and *E. coli* OX326A cells, respectively. We are also grateful to Prof. M. Ludwig and Ms. K. Pattridge for the coordinates of *E. coli* FeSOD. We finally thank Mr. M. Valentino for N-terminal protein sequence analysis and Mr. M. Farrugia for photographic assistance.

REFERENCES

Bannister, J. V., Bannister, W. H., & Rotilio, G. (1987) *Crit. Rev. Biochem. 22*, 111−180.

Beauchamp, C., & Fridovich, I. (1971) *Anal. Biochem. 44*, 276−287.

Benov, L., Chang, L. Y., Day, B., & Fridovich, I. (1995) *Arch. Biochem. Biophys. 319*, 508−511.

Benovic, J., Tillman, T., Cudd, A., & Fridovich, I. (1983) *Arch. Biochem. Biophys. 221*, 329−332.

Borgstahl, G. E. O., Parge, H. E., Hickey, M. J., Beyer, W. F., Jr., Hallewell, R. A., & Tainer, J. A. (1992) *Cell 71*, 107−118.

Bull, C., & Fee, J. A. (1985) *J. Am. Chem. Soc. 107*, 3295−3304.

Carlioz, A., Ludwig, M. L., Stallings, W. C., Fee, J. A., Steinman, H. M., & Touati, D. (1988) *J. Biol. Chem. 263*, 1555−1562.

Chan, V. W. F., Bjerrum, M. J., & Borders, C. L., Jr. (1990) *Arch. Biochem. Biophys. 279*, 195−201.

Cooper, J. B., Driessen, H. P. C., Wood, S. P., Zhang, Y., & Young, D. (1994) *J. Mol. Biol. 235*, 1156−1158.

Cooper, J. B., McIntyre, K., Badasso, M. O., Wood, S. P., Zhang, Y., Garbe, T. R., & Young, D. (1995) *J. Mol. Biol. 246*, 531−544.

Duke, M. V., & Salin, M. L. (1985) *Arch. Biochem. Biophys. 243*, 305−314.

Fee, J. A., McClune, G. J., Lees, A. C., Zidovetzki, R., & Pecht, I. (1981a) *Isr. J. Chem. 21*, 54−58.

Fee, J. A., McClune, G. J., O'Neill, P., & Fielden, E. M. (1981b) *Biochem. Biophys. Res. Commun. 100*, 377−384.

Halliwell, B., & Gutteridge, J. M. C. (1985) *Mol. Aspects Med. 8*, 89−124.

Hassan, H. M., & Fridovich, I. (1978) *J. Biol. Chem. 253*, 8143−8148.

Hopkin, K. A., Papazian, M. A., & Steinman, H. M. (1992) *J. Biol. Chem. 267*, 24253−24258.

Kanematsu, S., & Asada, K. (1979) *Arch. Biochem. Biophys. 195*, 535−545.

Klug-Roth, D., Fridovich, I., & Rabani, J. (1973) *J. Am. Chem. Soc. 95*, 2786−2790.

Laemmli, U. (1970) *Nature 227*, 680−685.

Lah, M. S., Dixon, M. M., Pattridge, K. A., Stallings, W. C., Fee, J. A., & Ludwig, M. L. (1995) *Biochemistry 34*, 1646−1660.

Lowry, O. M., Rosebrough, F., & Randall, R. J. (1951) *J. Biol. Chem. 193*, 265−275.

Ludwig, M. L., Metzger, A. L., Pattridge, K. A., & Stallings, W. C. (1991) *J. Mol. Biol. 219*, 335−358.

McAdam, M. E., Fox, R. A., Lavelle, F., & Fielden, E. M. (1977) *Biochem. J. 165*, 71−79.

McCord, J. M., & Fridovich, I. (1969) *J. Biol. Chem. 244*, 6049−6055.

Michalski, W. P., & Prowse, S. J. (1991) *Mol. Biochem. Parasitol. 47*, 189−196.

Parker, M. W., & Blake, C. F. (1988a) *FEBS Lett. 229*, 377−382.

Parker, M. W., & Blake, C. F. (1988b) *J. Mol. Biol. 199*, 649−661.

Parker, M. W., Blake, C. F., Barra, D., Bossa, F., Schinina, M. E., Bannister, W. H., & Bannister, J. V. (1987) *Protein Eng. 1*, 393−397.

Sambrook, J., Fritsch, E. F., & Maniatis, T. (1989) in *Molecular Cloning*: *A Laboratory Manual*, Cold Spring Harbor Labooratory Press, Plainview, NY.

Sanger, F., Nicklen, S., & Coulson, A. R. (1977) *Proc. Natl. Acad. Sci. U.S.A. 74*, 5463−5467.

Sevilla, F., Del Rio, L. A., & Hellin, E. (1984) *J. Plant Physiol. 116*, 381−387.

Shen, J., Subramaniam, S., Wong, C. F., & McCammon, J. A. (1989) *Biopolymers 28*, 2085−2096.

Sines, J., Allison, S., Wierzbicki, A., & McCammon, J. A. (1990) *J. Phys. Chem. 94*, 959−961.

Stallings, W. C., Powers, T. B., Pattridge, K. A., Fee, J. A., & Ludwig, M. L. (1983) *Proc. Natl. Acad. Sci. U.S.A. 80*, 3884−3888.

Stallings, W. C., Metzger, A. L., Pattridge, K. A., Fee, J. A., & Ludwig, M. L. (1991) *Free Radical Res. Commun. 12−13*, 259−268.

Steinman, H. (1982) in *Superoxide Dismutase* (Oberley, L. W., Ed.) Vol. I, pp 11−68, CRC Press, Boca Raton, FL.

Stoddard, B., Howell, P. L., Ringe, D., & Petsko, G. (1990) *Biochemistry 29*, 8885−8893.

Taylor, J. W., Ott, J., & Eckstein, F. (1985) *Nucleic Acids Res. 13*, 8764−8785.

Tierney, D. L., Fee, J. A., Ludwig, M. L., & Pennerhahn, J. E. (1995) *Biochemistry 34*, 1661−1668.

Wagner, U. G., Pattridge, K. A., Ludwig, M. L., Stallings, W. C., Werber, M. M., Oefner, C., Frolow, F., & Sussman, J. L. (1993) *Protein Sci. 2*, 814−825.

Weisiger, R. A., & Fridovich, I. (1973) *J. Biol. Chem. 248*, 4793−4796.

West, C. A., Bannister, J. V., Levine, B. A., & Perham, R. N. (1988) *Protein Eng. 2*, 307−311.

Ysebaert-Vanneste, M., & Vanneste, W. H. (1980) *Anal. Biochem. 107*, 86−95.

BI9629541